

See discussions, stats, and author profiles for this publication at:  
<https://www.researchgate.net/publication/222244320>

# Geometrical structure and nonlinear optical response of a zwitterionic push–pull biphenyl compound

ARTICLE *in* CHEMICAL PHYSICS · SEPTEMBER 2002

Impact Factor: 1.65 · DOI: 10.1016/S0301-0104(02)00723-1

CITATIONS

22

READS

23

## 6 AUTHORS, INCLUDING:



Alex Boeglin

University of Strasbourg

38 PUBLICATIONS 367 CITATIONS

SEE PROFILE



Fort Alain

Institut de Physique et Chimie des Mat...

135 PUBLICATIONS 2,352 CITATIONS

SEE PROFILE



L. Mager

French National Centre for Scientific R...

81 PUBLICATIONS 499 CITATIONS

SEE PROFILE



Vincent Rodriguez

University of Bordeaux

172 PUBLICATIONS 1,920 CITATIONS

SEE PROFILE

# Geometrical structure and nonlinear optical response of a zwitterionic push–pull biphenyl compound

A. Boeglin<sup>a,\*</sup>, A. Fort<sup>a</sup>, L. Mager<sup>a</sup>, C. Combellas<sup>b</sup>, A. Thiébault<sup>b</sup>, V. Rodriguez<sup>c</sup>

<sup>a</sup> IPCMS, Groupe d'Optique Non-Linéaire et d'Optoélectronique, CNRS UMR 7504, 23 rue du Loess, 67037 Strasbourg Cedex, France

<sup>b</sup> ESPCI, Environnement et Chimie Analytique, CNRS UMR 7121, 10 Rue Vauquelin, 75231 Paris Cedex, France

<sup>c</sup> Laboratoire de Physico-Chimie Moléculaire, 351 Cours de la Libération, 33405 Talence Cedex, France

Received 7 August 2001; in final form 8 January 2002

## Abstract

Solvent polarity effects on a disubstituted biphenyl have been investigated through IR, Raman, UV–visible spectroscopies. The results are interpreted in the light of some empirical and density functional electronic structures calculations. The vibronic structure has been determined and the normal modes in the finger print region have been assigned. This study opens the way to the exploitation of vibrational spectroscopy in the elucidation of the complex phenomena occurring when highly dipolar chromophores are embedded in dielectric media for applications in nonlinear optics (NLO). © 2002 Elsevier Science B.V. All rights reserved.

**Keywords:** Substituted biphenyls; Geometrical structure; Vibrational spectroscopy; Quadratic hyperpolarizability

## 1. Introduction

Organic molecules with intramolecular charge transfer states have been shown to be very promising candidates in quadratic nonlinear optics (NLO) [1]. Synthesis of push–pull polyenes with efficient donor acceptor groups can yield chromophores with very high static first-order hyperpolarizabilities [2,3]. Of course, for practical applications, some other parameters, such as thermal stability or optical transparency, have to be taken into account in the search for valuable

NLO chromophores and, for instance, preclude the use of conjugated systems with large spatial dimensions. Nevertheless, the progress achieved in the last few years has been driven by the improvement in our understanding of the relationships correlating molecular structure and linear/nonlinear optical properties. For polyenes in particular, the fact that the ground state polarity can be related to the bond length alternation (BLA), i.e. the average difference between the lengths of two adjacent carbon–carbon bonds, has proven to be of special importance in optimizing NLO properties for such molecules [4,5]. For push–pull compounds with more complex conjugation paths, the simple model based on the mixing of two resonance states of neutral and of charge transfer

\* Corresponding author.

E-mail address: alex.boeglin@ipcms.u-strasbg.fr (A. Boeglin).

characters [6] can be useful in interpreting experimental results as well [7,8].

Among the various NLO chromophores being studied, the biphenyl derivatives are of special interest due to the ability of the phenyl rings to rotate around the central C–C bond. This feature opens a specific route to modulate the charge transfer between the substituents by rotating one of the phenyl groups with respect to the other. Recent semi-empirical computational work by Ratner and co-workers [9] has shown the large dependence of the static quadratic hyperpolarizability on the twist angle between the two phenyl rings. This modulation is expected to be especially important for biphenyl compounds with zwitterionic character (molecules with a ground state dominated by the charge separated resonance form) since they possess a large ground state dipole moment and exhibit a large (negative) quadratic hyperpolarizability. We have selected such a zwitterionic molecule (4-(3,5-di-*tert*-butyl-4-oxidophenyl)-*N*-methylpyridinium), hereafter called PPP (para phenoxide pyridinium). The synthesis of this molecule (see Fig. 1) has been described previously [10]. The aim was to investigate the correlation between the twist angle and the linear, as well as nonlinear optical properties determined both experimentally and numerically.

To this end, we will exploit the fact that the geometric structure of the molecule is dependent on the local field due to the environment and hence can be modified by changing the polarity of the solvents used in the measurements. Indeed, it would be very demanding to try to control the angle of twist through steric crowding since the necessary chemical substitutions on the central carbon atoms are extremely difficult to carry out. Furthermore, chemical modifications that have already been tried tend to alter the electronic

structure of the chromophore making it difficult to draw conclusions. The replacement of the pyridinio group by a quinolinio group, for example, has already been investigated [11]. At that time, unfortunately, a tentative analysis of the geometrical structure by NMR measurements of the twist angle dependence on the solvent polarity was inconclusive because of the uncertainties inherent to the method. Instead we will rely here on techniques of vibrational spectroscopy to gain additional insights about the interaction between the PPP chromophore and various polar solvents as well as about the resulting changes in structural and electronic properties.

In this context, it is worth mentioning that the analysis of vibrational spectra has already been shown to be useful not only as a means towards structural characterization of conjugated molecular compounds but also as a way of determining the vibrational contributions to the molecular hyperpolarizabilities of acceptor–donor polyenes, for instance [12–15]. Furthermore, evidence has been presented that suggest these vibrational contributions correlate well with the purely electronic responses making it possible, at least in principle, to predict the NLO potential of push–pull chromophores from IR, Raman, and hyper Raman spectra [16]. More importantly, the simple two-state model for charge transfer molecules [6] can be extended to include linear electron–vibration coupling (Holstein model) in a self-consistent way that allows to recover some of the large environmental effects seen in electronic and vibrational spectra of these compounds [17].

In this work, we present the results of a series of experimental UV, IR, pre-resonance and near-resonance Raman spectra as well as quadratic hyperpolarizability measurements for the PPP molecule dissolved in solvents of different polarities. The experimental results are analyzed and compared to theoretical predictions obtained by various electronic structure calculations, both on the semi-empirical and *ab initio* (density functional) levels. The information we are able to gather in this way will be necessary to infer conclusions about the torsional motion between the two rings, a vibrational mode which is not readily accessible to experiments.

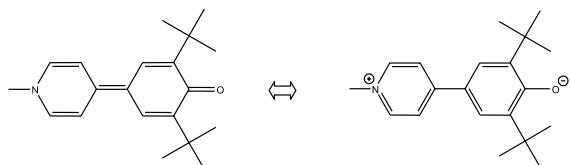


Fig. 1. Schematic representation of the two limiting resonance forms of PPP in a planar configuration.

## 2. Experimental results

### 2.1. Electronic processes

The UV–visible spectra have been recorded with a standard U6000 spectrometer. As seen in Fig. 2, the spectra reveal a rather smooth hypsochromic shift of the strong absorption band (the intra-molecular charge transfer band, or ICT for short) as a function of solvent polarity. We have chosen to represent this 500 nm band in units of wavenumbers to better size the vibronic progressions. The UV–visible spectra indeed show a very distinct vibronic structure for all the solvents with the exception of methanol. We have observed the same phenomena with ethanol, although, for the sake of clarity, we have not included it in Fig. 2. Therefore we can speculate that in alcohols, PPP is subjected to specific interactions with the solvent molecules which lead to a large inhomogeneous broadening of the ICT transition. Moreover, even with the greatest care being taken to avoid the presence of water in methanol, a weak absorption band remains at 350 nm corresponding to the protonated PPP molecule. In any of the solvents that we have used, the addition of water to the cell results in the disappearance of the 500 nm absorption band of PPP and in the appearance of the 350 nm band of its protonated form.

The optical quadratic nonlinearity of the molecule was determined by using the conventional

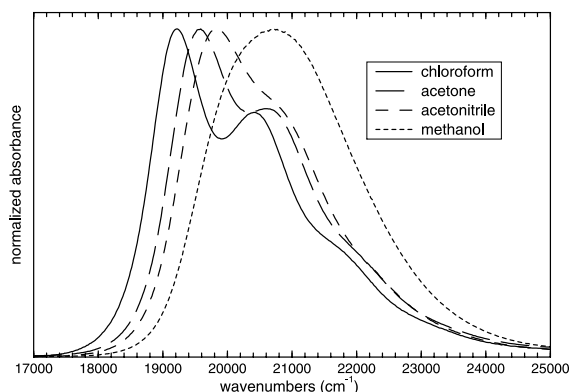


Fig. 2. UV–visible absorption spectra of PPP in four different solvents.

EFISH technique [18], especially suited for such push–pull rod-like molecules. The operating wavelength at 1.907  $\mu\text{m}$  was created by Raman shift of the 1.064  $\mu\text{m}$  *Q*-switched Nd:YAG light source. The measurements on the molecule in the different solvents used were calibrated relative to a quartz wedge whose quadratic susceptibility  $d_{11} = 1.2 \times 10^{-9}$  esu at 1.064  $\mu\text{m}$  was extrapolated to  $1.1 \times 10^{-9}$  esu at 1.907  $\mu\text{m}$ . Neglecting the nonorientational term, the technique determines the product  $\mu_g \beta(2\omega)$  where  $\mu_g$  stands for the permanent fundamental dipole moment and  $\beta(2\omega)$  for the quadratic hyperpolarizability at the harmonic laser pulsation  $\omega$ . In the two-level approximation valid for this molecule,  $\beta(2\omega)$  is one-dimensional along the charge transfer (CT) axis of the molecule and the static quadratic hyperpolarizability  $\beta(0)$  is deduced from a simple dispersion relation

$$\beta(2\omega) = \beta(0) \frac{\omega_{\text{CT}}^4}{(\omega_{\text{CT}}^2 - 4\omega^2)(\omega_{\text{CT}}^2 - \omega^2)},$$

$$\beta(0) = \frac{3\mu_{\text{eg}}^2(\mu_e - \mu_g)}{2\hbar\omega_{\text{CT}}^2},$$

where  $\hbar\omega_{\text{CT}}$  corresponds to the transition energy to the first excited CT state,  $\mu_{\text{eg}}$  to the electric dipole transition matrix element between the fundamental and the CT state and  $\mu_e$  to the dipole moment of the excited state.

The experimental results obtained in EFISH measurements on the PPP molecule dissolved in solvents of various polarities, are shown in Table 1. The zwitterionic character of the molecule reveals itself in the sign of the quadratic nonlinearities which are all negative. With increasing solvent

Table 1

Experimental  $\mu_g \beta$  results obtained from EFISH measurements for PPP in different solvents<sup>a</sup>

Solvents	$E_T$	$\lambda_{\text{CT}}$ (nm)	$\mu\beta(2\omega)$	$\mu\beta(0)$
$\text{CHCl}_3$	0.26	524	–325	–210
Acetone	0.36	512	–600	–400
Acetonitrile	0.46	503	–700	–470
Methanol	0.76	482	–900	–630

<sup>a</sup>  $E_T$  stands for the normalized parameter scaling the polarity of the solvents and  $\lambda_{\text{CT}}$  for the charge transfer absorption wavelength. The  $\mu_g \beta$  results are given in  $10^{-48}$  esu.

polarity, the high charge transfer character of the ground state is favored more and more. This leads to larger (in absolute value) nonlinearities with higher solvent polarities, as seen in Table 1. Apparently, none of the solvents is polar enough to push the chromophore structure far into its strongly charge separated form where the quadratic hyperpolarizability is predicted to vanish [6].

## 2.2. Vibrational spectroscopies

In order to probe the possible links between geometry and electronic properties, we have recorded a series of IR absorption spectra in various solvents. The mid-infrared measurements were performed on a Biorad interferometer (type FTS-60A) equipped with a globar source, a KBr beam splitter and a DTGS detector. Single beam spectra recorded in the spectral range 400–4000  $\text{cm}^{-1}$  with a 2  $\text{cm}^{-1}$  resolution were obtained by the Fourier transformation of 200 accumulated interferograms. Dilute solutions of PPP in different organic solvents (about 8 mg/ml) were injected between two KRS5 faces separated by a 200  $\mu\text{m}$  teflon spacer. For the sake of clarity, we present in Fig. 3 the IR difference spectra of PPP within four solvents only. Despite remnants of the very strong and dense absorption bands of the polar solvents in the 1400  $\text{cm}^{-1}$  region which have been suppressed, we can clearly identify five main absorption bands for PPP in the finger print region from

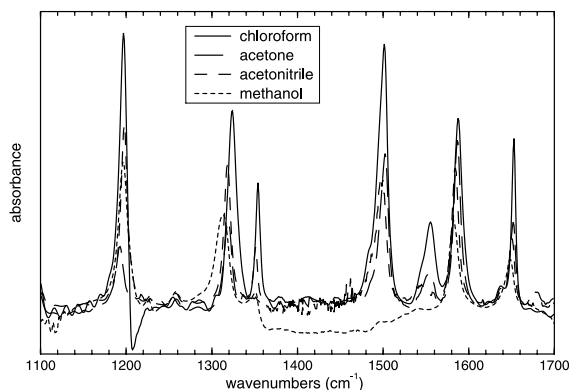


Fig. 3. Infrared absorption spectra of PPP in four different solvents.

1100 to 1700  $\text{cm}^{-1}$ . We notice strong changes in the relative intensities between these bands depending on the solvents. In some cases, and this is especially true for the 1300  $\text{cm}^{-1}$  band, we detect sizeable shifts in frequencies as well as a strong broadening. It is from these features that one can hope to gain some insights into the changes in structures that the solute molecules undergo in contact with the various solvents.

We have furthermore recorded unpolarized Raman spectra (1100–1700  $\text{cm}^{-1}$ ) in the backscattering geometry on a Labram I (Dilor-France) microspectrometer in conjunction with a confocal microscope (50 $\times$  objective). A CCD was used for detection and 752.5 nm radiation from a  $\text{Kr}^+$  laser was selected to record pre-resonance Raman spectra of PPP in several solvents. The resulting difference spectra between pure solvent and solution are shown in Fig. 4. The alignment and calibration of the optical elements were checked by recording the intense Raman signal at 521  $\text{cm}^{-1}$  of a silicon plate. The precision of the wavenumber measurements was  $\pm 0.5 \text{ cm}^{-1}$  and the resolution about 4  $\text{cm}^{-1}$ . Finally, using an  $\text{Ar}^+$  laser source at 514.5 nm, we also recorded a near-resonant spectrum of the molecule in methanol. The curve shown in Fig. 5 corresponds to the light scattered by the solution and not to a difference spectrum as done previously in Fig. 4. This shows therefore a strong enhancement of the 1300  $\text{cm}^{-1}$  band under these near-resonant excitation conditions indicating that

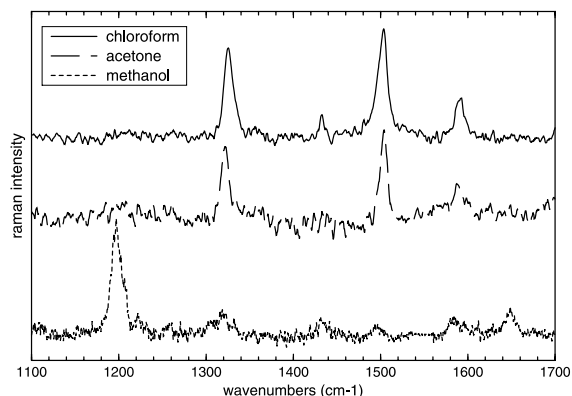


Fig. 4. Pre-resonant (752.5 nm) Raman spectra of PPP in different solvents.

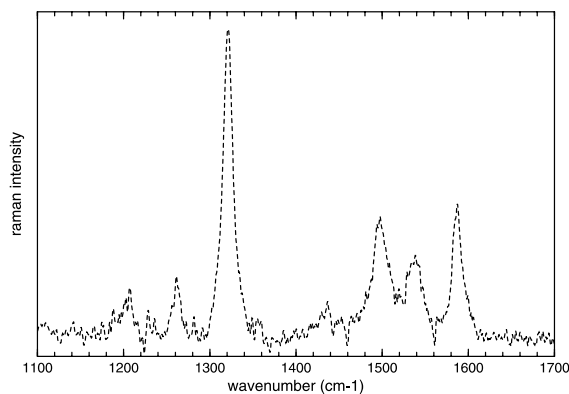


Fig. 5. Near-resonant (514.5 nm) Raman spectra of PPP in methanol.

this mode is optically active in the electronic transition to the excited state.

### 3. Computational results and interpretation

#### 3.1. Computational techniques

We have used different computational approaches to evaluate PPP properties of interest. On the semi-empirical level, the MOPAC6 code, with the AM1 parameters [19], has been used to optimize the geometries and to evaluate the static hyperpolarizabilities. The ZINDO code, with INDO1 parameters [20], has been used to determine the excited states, the transition dipole moments, as well as changes in permanent dipole moments upon excitation.

On the *ab initio* level, the DMol3 code<sup>1</sup> has been exploited for both geometry optimizations and normal mode analysis with evaluation of infrared absorption intensities. The nonlocal density approximation with the generalized gradient corrected functional by Perdew and Wang [21] and polarization basis sets were used.

<sup>1</sup> Dmol3 is a registered software product of Molecular Simulations Inc., the graphical displays were from the Cerius2 molecular modeling system.

#### 3.2. Geometrical structure

The geometries of the isolated PPP molecule have been obtained through both the semi-empirical AM1 hamiltonian and the *ab initio* density functional. In both instances, the predicted geometries are either planar or slightly twisted ( $2.8^\circ$ ). They correspond to the quinoid structure depicted on the left-hand side of Fig. 1. This result is surprising since biphenyl compounds are known to adopt a twisted configuration [22]. One can always impose a finite twist angle, however, when using the AM1 hamiltonian, the angle has to be sufficiently large in order to observe sizeable changes in bond lengths as shown in Fig. 6(a). Alternatively, using the density functional method, we can optimize the geometry in an external electric field. We observe that a field strength of about 0.01 in atomic units is needed to alter the bond lengths significantly, as shown in Fig. 6b. Notice that the twist angle increases only moderately from  $2.8^\circ$  to  $11.5^\circ$  in the process. In both instances, the lengthening of the double bonds and the shortening of the single bonds seem to be essential to bring

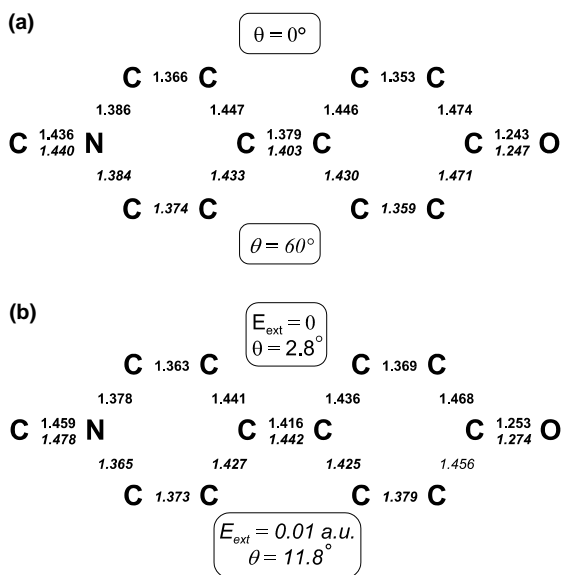


Fig. 6. Bond lengths in PPP as obtained (a) with MOPAC (AM1 hamiltonian) for the planar geometry and for a fixed twist angle of  $60^\circ$  and (b) with DMol3 (GGA functional) without and with an applied electric field of 0.01 a.u.

the evaluated properties into rough agreement with the experimental measurements.

When performing finite field calculations of the first-order hyperpolarizability of PPP in the gas phase with MOPAC, comparable values for the product  $\mu_g\beta$  can only be obtained if one imposes the constraint of rather large twist angles between the pyridine and the phenoxide rings [23]. These results are in total agreement with the work of Ratner and co-workers [9] who used a summation over (excited) states (SOS) technique which they devised and implemented into the ZINDO package. Our own computations with the INDO1 parameters show that in the planar geometry the dipole moments of the ground and first excited states as well as the transition dipole moment are all about 11 Debye. As the twist angle is increased to  $60^\circ$ , the ground state becomes more polar leading to a  $\Delta\mu$  value of about 8 Debye, while the transition dipole moment changes by less than 1 Debye only. It is this increase in  $\mu$  and  $\Delta\mu$  with the twist angle which makes it possible to bring the computed nonlinearities in line with the experimental results of Table 1, whereas, within the solvent, the charge transfer from the nitrogen to the oxygen atom is being stabilized by the dielectric medium.

### 3.3. Vibrational normal modes

In order to assign these bands, we have used normal mode calculations based on the density functional theory as implemented in the DMol3 software. The results are shown in Fig. 7. The

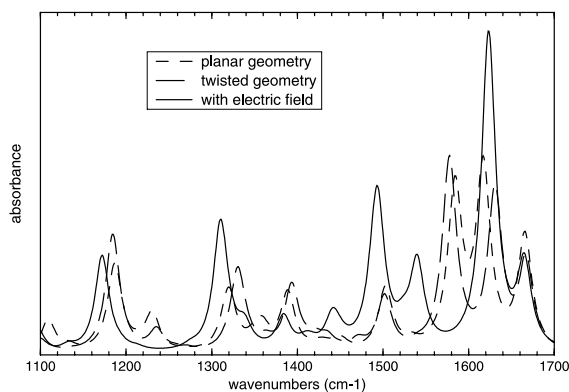


Fig. 7. Simulated infrared spectrum of PPP.

geometry optimization leads to a nearly planar configuration for the molecule. In this planar geometry, the two bands above  $1600\text{ cm}^{-1}$  correspond to coupled stretches within the pyridine and phenyl rings. Right below  $1600\text{ cm}^{-1}$  we find a vibrational mode dominated by the C–O stretch. The three absorption bands between  $1300$  and  $1500\text{ cm}^{-1}$  all involved the inter-ring C=C stretch. The C–N stretch appears around  $1200\text{ cm}^{-1}$ .

Identical computation have been performed with an external electric field of 0.01 atomic units to mimic a solvent reaction field. In this case, the geometry optimization leads to an internal twist angle of  $11.5^\circ$ . The intensities of the ring motions above  $1600\text{ cm}^{-1}$  are strongly perturbed. The C–O stretch is shifted down to  $1540\text{ cm}^{-1}$  and its intensity falls off sharply. Most of its intensity and some of the C–O motion is transferred to the  $1500\text{ cm}^{-1}$  mode. The central ring stretch at  $1300\text{ cm}^{-1}$  doubles in intensity while the C–N stretch shifted down to  $1180\text{ cm}^{-1}$ . Finally, keeping the twist angle frozen at  $11.5^\circ$ , we have re-optimized the geometry and determined the normal modes vibrations without an applied electric field. As shown in Fig. 4, this leads to a computed IR spectrum very similar to the one obtained in the planar geometry.

Although the level of sophistication of our simulations may not be the highest possible and our results may not reproduce the energies and respective intensities of all the bands very accurately, we believe that the normal modes are at least given in the right order. Nevertheless, the simulations in a finite electric field lead to a close similarity with the experimental spectra for the bands at  $1200$ ,  $1300$ , and  $1500\text{ cm}^{-1}$ .

### 3.4. Bands assignments

We therefore propose the following assignment for the IR bands featured in Fig. 3, using the Wilson notation [24]. The band at  $1590\text{ cm}^{-1}$  corresponds mainly to the quinoidal double bond stretch of the phenoxide group. At  $1650\text{ cm}^{-1}$  we observe the analogous stretching mode for the pyridinium group. To be more specific, we should add that the  $1590\text{ cm}^{-1}$  mode contains also an in-phase contribution of the pyridinium stretch and is

therefore a relative of the 8a mode of biphenyls. In the same way, the  $1650\text{ cm}^{-1}$  mode is the anti-symmetric combination of the two contributions. This is consistent with the Raman spectra at 514 nm (Fig. 5) and at 752.5 nm (Fig. 7) of PPP in methanol. While the resonant scattering process leads to the observation of the  $1590\text{ cm}^{-1}$  peak only, the pre-resonant regime allows to detect a trace of the  $1650\text{ cm}^{-1}$  mode. The results of numerical simulations put the symmetric benzoquinone dominated stretch mode at  $1620\text{ cm}^{-1}$ , while the asymmetric double bond stretches are at  $1561\text{ cm}^{-1}$ . This splitting is slightly smaller than the one observed in *p*-benzoquinodimethane already observed for the symmetric ( $1621\text{ cm}^{-1}$ ) and asymmetric ( $1536\text{ cm}^{-1}$ ) modes [25]. Notice that this asymmetric mode is not IR active.

Next, the IR and Raman active band at  $1500\text{ cm}^{-1}$ , can be ascribed to the in-phase mode 19a which involves mainly coupled stretches between the pyridine and the phenyl rings. However, the observed strong IR and weak Raman intensities are consistent with an in-phase contribution of the carbonyl group mode as indicated by our numerical simulations. Around  $1320\text{ cm}^{-1}$ , we find the central C–C stretching mode 13 [26], the one that should be most sensitive to changes in the intraring twist angle [22]. Indeed, this band displays the largest shifts in energy as a function of solvent polarity:  $1326\text{ cm}^{-1}$  in chloroform,  $1322\text{ cm}^{-1}$  in acetone,  $1321\text{ cm}^{-1}$  in acetonitrile, and  $1319\text{ cm}^{-1}$  in methanol as determined by Raman spectroscopy. This mode is also the one that is responsible for the vibronic structure observed in the UV–visible spectra as can be verified from a numerical fit using Frank and Condon factors for displaced and distorted oscillators. Hence, it is not surprising that this vibrational band is subjected to strong inhomogeneous broadening in methanol as can be seen in Figs. 3 and 4. Finally, the band at  $1200\text{ cm}^{-1}$  involving the methyl-N stretch can be ascribed to mode 9a.

#### 4. Conclusions

Para-substituted biphenyls are generally thought of as presenting a torsional angle of about

$30^\circ$  [27]. The signature vibration band of the central C–C stretch usually lies between  $1280$  and  $1300\text{ cm}^{-1}$  [26]. For the PPP chromophore that we have studied here, a frequency over  $1320\text{ cm}^{-1}$  hints to a lower twist angle than expected, especially in view of the semi-empirical quadratic hyperpolarizability calculations compared to experimental values.

The frequency shifts of the mode with respect to solvent polarity are well established, especially with the micro-RAMAN set-up, where the measurements are precise to within  $0.5\text{ cm}^{-1}$ , as opposed to the  $2\text{ cm}^{-1}$  of the Fourier transform IR spectrometer. The total shift of about  $7\text{ cm}^{-1}$  correlates with a change of  $\mu_g\beta(0)$  by almost a factor of 4. This points towards potentially large increases in quadratic hyperpolarizabilities, under torsion of the conjugation path, e.g. through steric hindrance. This strengthens the conclusions drawn from semi-empirical calculations although they are plagued by geometrical structure problems.

The results of vibrational spectroscopy presented here open the way to the applications of this technique to the study of nonlinear chromophores embedded in different dielectric media, such as polymers for example. The micro-RAMAN technique seems especially well suited for the study of environmental effects using push–pull molecules as a sensitive probe in other media than solutions.

#### References

- [1] J. Zyss, I. Ledoux, J.-F. Nicoud, *Molecular Nonlinear Optics*, Academic Press, New York, 1994.
- [2] M. Ahlheim, M. Barzoukas, P.V. Bedworth, M. Blanchard-Desce, A. Fort, Z.-Y. Hu, S.R. Marder, J.W. Perry, C. Runser, M. Staehlin, B. Zysset, *Science* 271 (1996) 335.
- [3] M. Blanchard-Desce, V. Alain, L. Midrier, R. Wortmann, S. Lebus, C. Glania, P. Krämer, A. Fort, J. Muller, M. Barzoukas, *J. Photochem. Photobiol. A: Chem.* 105 (1997) 105.
- [4] S.R. Marder, C.B. Gorman, F. Meyers, J.W. Perry, G. Bourhill, J.-L. Brédas, B.M. Pierce, *Science* 265 (1994) 632.
- [5] F. Meyers, S.R. Marder, B.M. Pierce, J.-L. Brédas, *J. Am. Chem. Soc.* 116 (1994) 10703.
- [6] J.-L. Oudar, D.S. Chemla, *J. Chem. Phys.* 66 (1977) 2664; J.-L. Oudar, *J. Chem. Phys.* 67 (1977) 446.
- [7] M. Barzoukas, C. Runser, A. Fort, M. Blanchard-Desce, *Chem. Phys. Lett.* 257 (1996) 531.
- [8] M. Barzoukas, A. Fort, M. Blanchard-Desce, *New J. Chem.* 21 (1997) 309.



- [9] I.D. Albert, T.J. Marks, M.A. Ratner, *J. Am. Chem. Soc.* 120 (1998) 1174.
- [10] G. Bacquet, P. Bassoul, C. Combellas, J. Simon, A. Thiébault, F. Tournilhac, *Adv. Mater.* 2 (1990) 311.
- [11] C. Runser, A. Fort, M. Barzoukas, C. Combellas, C. Suba, A. Thiébault, R. Graff, J.-P. Kintzinger, *Chem. Phys.* 193 (1994) 309.
- [12] D.M. Bishop, *Adv. Chem. Phys.* 104 (1998) 1.
- [13] M. Del Zoppo, C. Castiglioni, P. Zuliani, G. Zerbi, in: *Handbook of Conducting Polymers*, Marcel Dekker, New York, 1998, p. 765.
- [14] C. Castiglioni, M. Tommasini, M. Del Zoppo, *J. Mol. Struct.* 512 (2000) 137.
- [15] M. Tommasini, C. Castiglioni, M. Del Zoppo, G. Zerbi, *J. Mol. Struct.* 480 (1999) 179.
- [16] M. Del Zoppo, *Vib. Spectrosc.* 24 (2000) 63, and references herein.
- [17] A. Painelli, *Chem. Phys. Lett.* 285 (1998) 352; A. Painelli, F. Terenziani, *Chem. Phys. Lett.* 312 (1999) 211; A. Painelli, *Chem. Phys.* 245 (1999) 185.
- [18] See Ref. 6 and also T. Thami, P. Bassoul, M.A. Petit, J. Simon, A. Fort, M. Barzoukas, A. Villaeys, *J. Am. Chem. Soc.* 114 (1992) 915.
- [19] J.J.P. Stewart, *J. Comput. Chem.* 10 (1989) 209.
- [20] J. Ridley, M.C. Zerner, *Theor. Chim. Acta* 32 (1973) 111; A.D. Bacon, M.C. Zerner, *Theor. Chim. Acta* 53 (1979) 21.
- [21] J.P. Perdew, Y. Wang, *Phys. Rev. B* 45 (1992) 13244.
- [22] G. Zerbi, S. Sandroni, *Spectrochim. Acta A* 24 (1968) 483; G. Zerbi, S. Sandroni, *Spectrochim. Acta A* 24 (1968) 511.
- [23] A. Fort, A. Boeglin, L. Mager, C. Amyot, C. Combellas, A. Thiébault, V. Rodriguez, *Synth. Met.* 124 (2001) 209.
- [24] E.B. Wilson, *Phys. Rev.* 45 (1934) 706.
- [25] Y. Yamakita, M. Tasumi, *J. Phys. Chem.* 146 (1995) 8524.
- [26] C. Didierjean, V. De Waele, G. Buntix, O. Poizat, *Chem. Phys.* 237 (1998) 169; G. Buntix, R. Naskrecki, C. Didierjean, O. Poizat, *J. Phys. Chem. A* 101 (1997) 8768.
- [27] R.M. Roberts, *Magn. Reson. Chem.* 23 (1985) 52.